Experimental study on a novel foaming formula for CO_2 foam flooding

X. Xu[*, 1], A. Saeedi[1] and K. Liu [2]

[1] Department of Petroleum Engineering, Curtin University, Perth 6151, Australia

[2] Research Institute of Petroleum Exploration & Development, Beijing 100083, China

ABSTRACT

This research developed a viable and economical foaming formula (AOS/AVS/N70K-T) which is capable of creating ample and robust CO_2 foams. Its foaming ability and displacement performance in a porous medium was investigated and compared with the two conventional formulations (AOS alone and AOS/HPAM). The results showed that the proposed formula could significantly improve the foam stability without greatly affecting the foaming ability, with a salinity level of 20,000 ppm and a temperature of 323K. Furthermore, AOS/AVS/N70K-T foams exhibited thickening advantages over the other formulations, especially where the foam quality was located around the transition zone. This novel formulation also showed remarkable blocking ability in the resistance factor (RF) test, which was attributed to the pronounced synergy between AVS and N70K-T. Last but not the least, it was found that the tertiary oil recovery of the CO_2 foams induced by AOS/AVS/N70K-T was 12.5 % higher than that of AOS foams and 6.8% higher than that of AOS/HPAM foams at 323K and 1500 psi, thus indicating its huge EOR potential. Through systematic research, it is felt that the novel foaming formulation might be considered as a promising and practical candidate for CO_2 foam flooding in the future.

Keywords: CO_2 foam flooding, foamability and foam stability, apparent foam viscosity, foam blockage, accumulative oil recovery

1. INTRODUCTION

Among the gases which can be applied in the gas flooding process, CO_2 is considered the most commonly used source worldwide [1-4]. It is capable of forming a dense or supercritical phase with the characteristic of high density and high viscosity in typical reservoir conditions, and this feature significantly facilitates its miscibility with the crude oil [5-7]. Another advantage of dense CO_2 as a displacement fluid is its extremely low solubility in formation water, preventing an excessive amount of the CO_2 from being lost when CO_2 flooding is performed in water-flooded reservoirs. Moreover, capturing and injecting CO_2 into the petroleum-bearing underground will greatly reduce the greenhouse gas (GHG) effect as well as produce oil, which also makes the CO_2 flooding a compelling enhanced oil recovery (EOR) strategy [8-10].

Despite its huge potential for ongoing oil production worldwide, CO_2 flooding possesses a number of weaknesses as an EOR technique, such as viscous fingering and gravity segregation, which may lead to early CO_2 breakthrough and a low recovery factor [11, 12]. Therefore, numerous investigations have been carried out to improve the displacement performance of the CO_2 flooding over the past few decades [13-15]. Among these techniques, the use of foamed CO_2 is believed to offer the best hope due to its exceptional capability of controlling CO_2 mobility which, accordingly, enables more areas to be swept by the CO_2 flooding. With regards to this method, the primary concern is that the injected foam may collapse in the presence of crude oil or under harsh reservoir conditions, which detrimentally affect the displacement efficiency of the liquid being displaced [16]. There have been extensive attempts made to promote the foam stability, and two main categories are involved [17-20]: nanoparticle-stabilized foam and polymer-enhanced foam. However, the former is not economical and may cause long-term health effects, while the latter is not sufficiently robust due to the polymer degradation moreover, the existence of the polymer results in

tremendous foamability loss.

This research presents a viable and economical EOR method which introduces the mixture of additives into the foaming solution to stabilize CO_2 foam during CO_2 foam flooding. Initially, investigations were carried out to screen a novel foaming formulation with the potential to provide a good balance of foamability and foam stability. Then, special attention was given to the core flooding experiment allowing studies of apparent foam viscosity, resistance factor (RF) and residual resistance factor (RRF), as well as the accumulative oil recovery under relatively harsh reservoir conditions. Section 2 shows the materials, experimental setup and procedures to be applied in this study. Section 3 presents the results of the static and dynamic performance of the enhanced CO_2 foam. Discussions and interpretations have also been included in this section. The paper ends with with the concluding remarks in Section 4.

2. EXPERIMENTAL SECTION

2.1 Materials. Triton X-100, APG C12-16, Sodium dodecyl sulfate (SDS), triethanolamine, $CaCl_2$ and NaCl were supplied by Sigma-Aldrich Co., Ltd (Australia); Sodium alpha olefin sulfate (AOS C14-16) with 35% active matter was obtained from Stepan Chemical Co. (USA). Additive N70K-T was purchased from Solvay Chemicals Inc. (USA); HPAM was provided by Beijing Hengju Chemical Co., Ltd (China), with a molecular weight of 2.5×10^7 g/mol and a hydrolysis degree of 25%; AVS which was a ter-polymer of acrylamide (AM), AMPS and one synthesized functional monomer was provided by the Research Institute of Petroleum Exploration & Development (RIPED, China). The schematic of HPAM and AVS molecules are illustrated in Fig. 1. Berea samples with length around 6.9 cm and diameter of 3.8 cm were cut from quarried sandstone blocks (Ohio, USA) and used as supplied. Their compositions were determined by X-ray powder diffraction (XRD) and were tabulated in Table 1. Oil sample is sourced from an oil reservoir located on North West Shelf

of Western Australia and its properties are listed in Table 2. CO_2 gas with 99.99% purity was supplied by BOC (Australia) and applied throughout the entire research process.

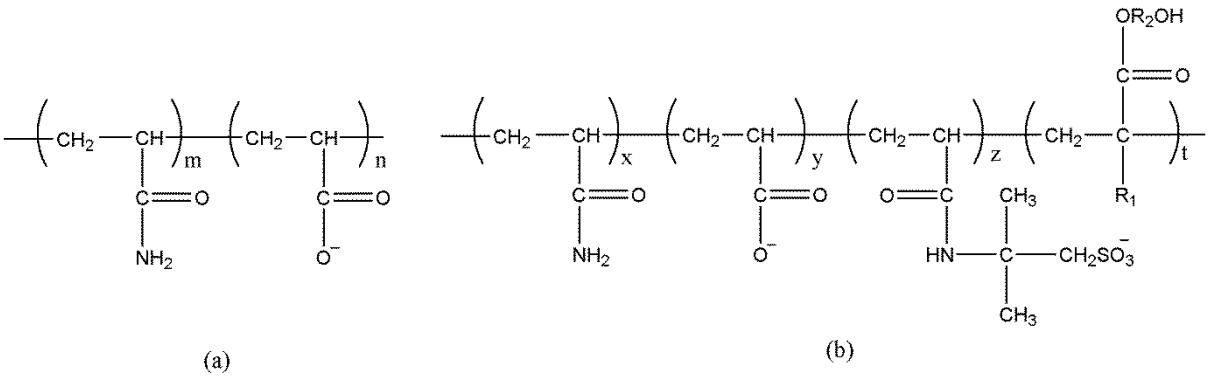

Fig. 1 Schematic of HPAM (a) and AVS (b) molecular structure

Table 1 The oxides composition of the core plug

Oxide	SiO_2	CaO	CO_2	Na_2O	Al_2O_3	H_2O	MgO	K_2O
Weight%	83.15	2.15	2.44	0.09	3.45	0.14	1.12	1.59

Table 2 Properties of the Crude Oil

Test	Unit	Result
Density @ 15°C	Kg/L	0.9428
API gravity	°API	18.5
Asphaltenes	%mass	0.14
Arsenic	mg/kg	2.3
Kinematic Viscosity @40°C	cSt	37.26
Sulphur-Total	%mass	0.14
Total Acid Number	mg KOH/g	0.50
Water Content	%volume	0.150

2.2 Experimental procedures. *2.2.1 Foaming ability and foam stability*. Two nonionic surfactants Triton X-100 and APG along with two anionic alternatives AOS and SDS were chosen as the foaming agents. Either polymers or other additives were used as thickeners to stabilize the CO_2 foam. As a result of its simplicity and reliability, the Waring blender method [21] was selected for this research investigating foamability and foam stability in order to determine whether a reliable and robust foam could be generated or not.

Synthetic formation water containing 20,000 ppm NaCl and 100 ppm $CaCl_2$ was employed to prepare the foaming solution in the experiments. Firstly, 100 mL solution of foaming agent/thickener was added into the Warring blender and agitated at a speed of 2000 rpm for 60 seconds with continuous CO_2 gas injection. The foam produced was then transferred to a graduated cylinder which was standing in a water bath, the temperature of which was controlled by a digital thermal couple. The initial volume (V_0) of generated foam was measured as foamability and the time period ($t_{1/2}$) for half of the liquid dropout (i. e. the liquid drainage volume reached 50 mL) was recorded as foam stability under various test conditions. All the tests were conducted at 323K unless otherwise specified.

2.2.2 Foam apparent viscosity. On the basis of single-phase Darcy law, the apparent foam viscosity can be expressed as:

$$\mu_{foam,app} = \frac{\mathrm{kA\Delta p}}{(q_g + q_l)L} \quad \ldots\ldots\ldots\ldots\ldots\ldots\ldots\ldots\ldots\ldots \quad (1)$$

where k is the effective permeability of the core plug, A is the cross section to foam flow, q_g and q_l are the volumetric flow rates of CO_2 gas and foaming solution respectively, and $\Delta p/L$ is the pressure gradient across the full length of the core plug. The experimental setup is illustrated in Fig. 2. Foaming solution (5.0 PV) was fed into the core plug to satisfy the surfactant adsorption before the injection of the CO_2 foam which was produced with the assistance of a foam generator (Haian Oil Scientific Research Apparatus Co., Ltd., China). Illustration of the foam generator is given in Fig. 3. The differential pressure at different times during the experiment was monitored and recorded by pressure transducers (KELLER, Switzerland) mounted at the inflow and outflow end of the core holder. Gas/ liquid ratio (foam quality) would not be altered until steady state flow was achieved, which was indicated by negligible fluctuation (less than 5 psi) of pressure drop. The temperature controlled by the

heating tape and the pressure controlled by a back pressure regulator (BPR) were maintained at 323K and 10.3 MPa respectively in the experiments.

2.2.3 Resistance factor (RF) and residual resistance factor (RRF). If both formation water (brine) and foam flow in the same core sample at same flow rate, the definition of RF can be simplified as:

$$R = \frac{\Delta p_2}{\Delta p_1} \quad \text{(2)}$$

where $\Delta p_1 and\ \Delta p_2$ are the pressure drops of brine flow and foam flow, respectively.

Similarly, if brines flow at the same rate, RRF can be calculated by:

$$RRF = \frac{\Delta P_3}{\Delta P_1} \quad \text{(3)}$$

where $\Delta p_1 and\ \Delta p_3$ are the pressure drops of brine flow before and after foam flooding respectively.

The experimental setup is illustrated in Fig. 2. Prior to the measurement, a sufficient amount of foaming solution (5.0 PV) was fed into the core plug to meet the demand of surfactant adsorption. Then synthetic formation water (NaCl 20,000 ppm and $CaCl_2$ 100 ppm) was injected at 1.0 mL/min until steady ΔP_1 was reached. Next CO_2 and a foaming solution were injected into the sample after passing through a foam generator with the flow rates of 0.75mL/min and 0.25 mL/min respectively (foam quality was 75%). The injection shifted to brine again flowing at 1.0 mL/min after steady $\Delta p_2$was obtained, and then brine flow continued until ΔP_3 could be measured. All the experiments were conducted at 323K and 10.3 MPa.

2.2.4 Accumulative oil recovery. To evaluate the recovery of CO_2 foam flooding induced by different formulations, oil displacement assessments were conducted. The procedures were as follows: After the petrophysics properties of the core were determined, the core was fully saturated with brine. Then crude oil was injected into the core until the water cut reached 1%. The sample was aged for 24 hours and then water flooding was conducted to obtain residual oil saturation, which was followed by a 1 PV (pore volume) foam slug and extended water floods until water cut was greater than 99%. The system temperature and pressure were maintained at 323K and 10.3 MPa throughout the core flooding tests.

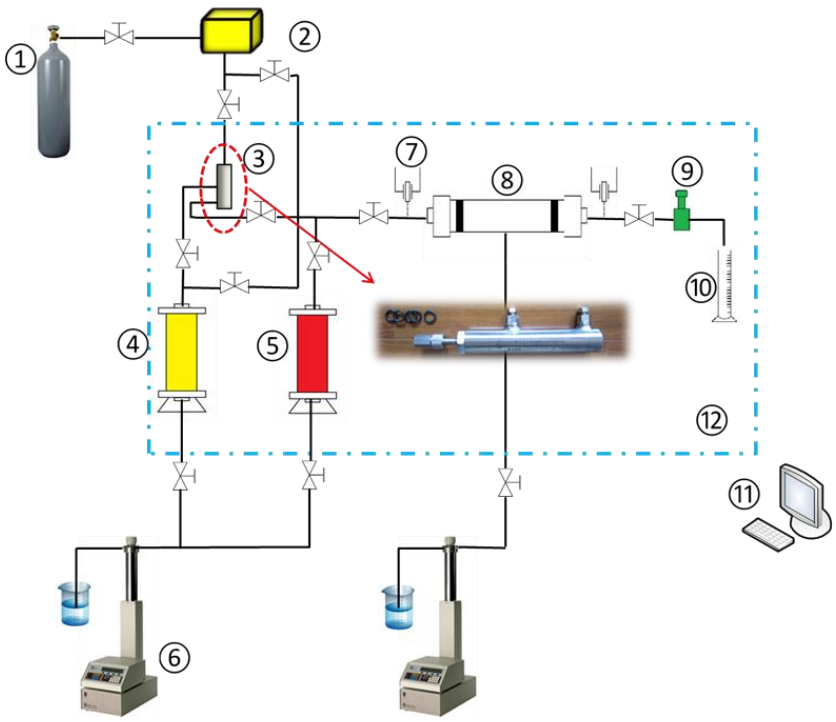

Fig. 2 Experimental schematic of the foam performance evaluation (apparent foam viscosity, RF and RRF, oil displacement)

1- CO_2 Tank 2- Gas Mass Flow Control System 3- Foam Generator 4- Chemical Solution 5- Sythetic brine 6- Injection Pump 7- Pressure Transducer 8- Core Holder 9- Back Pressure Regulator 10- Graduated Cylinder 11- Data Acquisition System 12- Heating System

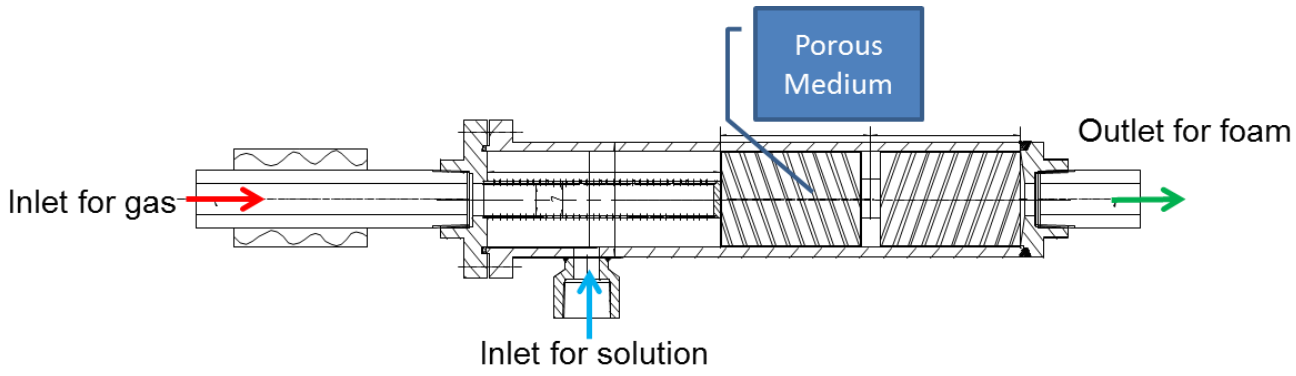

Fig.3 The schematic of the foam generator

3. RESULTS AND DISCUSSION

3.1 Screening of foaming solution. *3.1.1 Determination of foaming.* The static foam behavior was strongly related to the type and concentration of the foaming agent (most of them were surfactants), which can be verified by the results shown in Fig. 4-7. It was noted that the concentration was based on the active substance of these surfactant products. In general, nonionic surfactants (Triton X-100 and APG) generated less foam than the counterpart anionic surfactants (AOS and SDS) under both low and high concentrations. In the case of Triton X-100, its foamablity fluctuated with a maximum of only 380 mL which hardly satisfied the foaming requirement, and the stability which varied between 84s and 123s was at the peak under the concentration of 0.4 w.t.%; on the other hand, the scenario of APG, one highly attractive “green surfactant” due to its remarkable biodegradability, was quite different: the foamability rose smoothly as surfactant concentration increased and the growth rate was nearly constant throughout the test; however, it was deemed not suitable under the test conditions/based on the outcome of the tests if insufficient foam creation was taken into consideration. Interestingly, although an abundant amount of foam could not be obtained, the foam generated by APG was relatively robust and stable thanks to its

extraordinary bulk viscosity. Accordingly, it could be considered as the best candidate among the foaming agents investigated in terms of the stability, but poor foamability hampered its possible application for foam flooding.

As expected, AOS and SDS, which were anionic foaming agents, exhibited exceptional foaming ability. The foamability of AOS increased rapidly at low concentration before reaching a plateau (around 620 mL) after which the foamability started dropping slightly. In contrast to AOS, foamability of SDS increased with surfactant concentration during the course of the experiment and it was a bit higher than that of AOS under the same concentration. However, with regard/when it came to foam stability, the scenario was completely the opposite: AOS performed much better than its counterpart/alternative SDS within the whole range of concentrations investigated, and this tendency became noticeable as the concentration rose. The foam stability disparity between the two candidate solutions could be partially explained by the huge difference in bubble size distribution. Fig. 8 was captured by a digital camera (Lenka, Germany) and visually demonstrates the bubble size distribution of foams generated by AOS and SDS (0.5 wt. %) over 600 s. The corresponding bubble size distributions were measured and calculated by using image analysis software (Nano Measurer 1.2, Fudan University), and the results are quantitatively shown in Fig. 9-10. Monsalve and Schechter concluded [22] that longer foam lifetime is associated with narrower bubble size distribution; that is, smaller variances favored the foam stability. In this experiment, it was observed that the initial bubble diameter of foams produced by these two foaming agents was highly uniform and this indicated both bubble size distributions were narrow right after the generation of foam, with the average bubble diameters of AOS foam and SDS foam being 45 μm and 80 μm, respectively. Although it could be expected that the distribution would vary over time, the distributions of AOS foam and of SDS foam changed in a different manner after 600 s: the bubble size of the former was still distributed relatively

narrowly with around 70% of its bubbles sitting in the range of 125μm and 180 μm, while the bubble size distribution of the latter became much wider than before, which can be validated by image 12, where bubbles with various diameters are stacked together. Furthermore, on the basis of Laplace's equation, smaller bubbles tend to coalesce into larger ones owing to the capillary pressure difference, leading to dramatic foam stability reduction.

Therefore, it could be concluded that AOS was the best foaming agent among these alternative formulations under the test conditions. Taking into account the foamability and stability equally/giving equal weight (or importance) to foamability and stability, 0.5 wt. % was chosen as the foaming agent concentration unless otherwise specified.

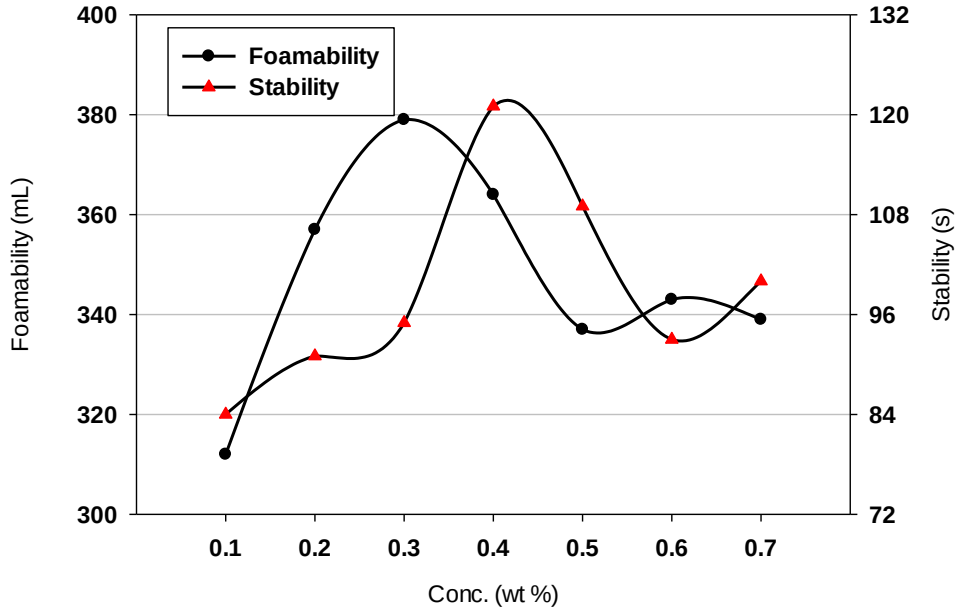

Fig. 4 The dependence of foamability and foam stability on Triton X-100 concentration

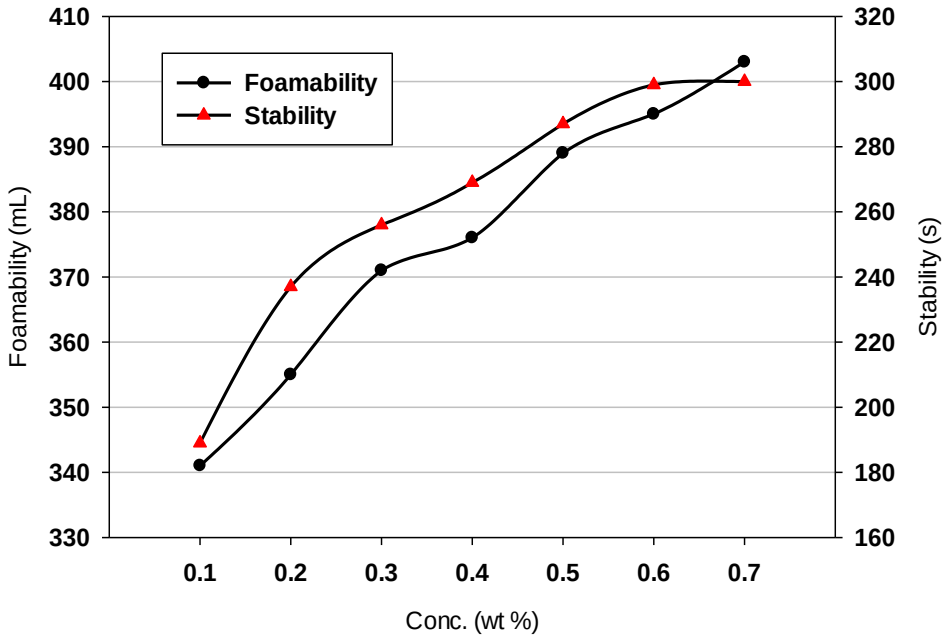

Fig. 5 The dependence of foamability and foam stability on APG concentration

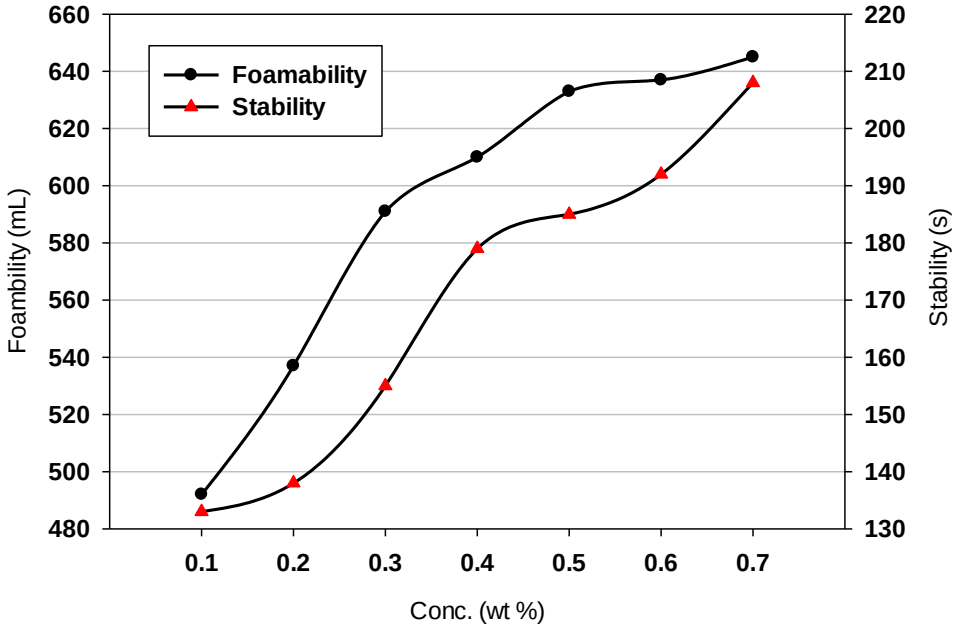

Fig. 6 The dependence of foamability and foam stability on SDS concentration

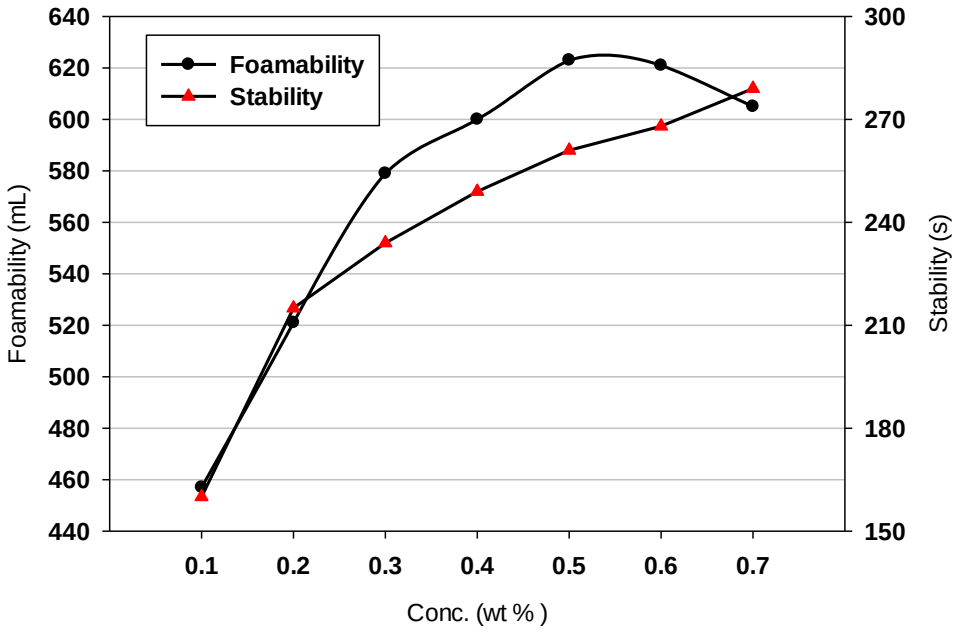

Fig. 7 The dependence of foamability and foam stability on AOS concentration

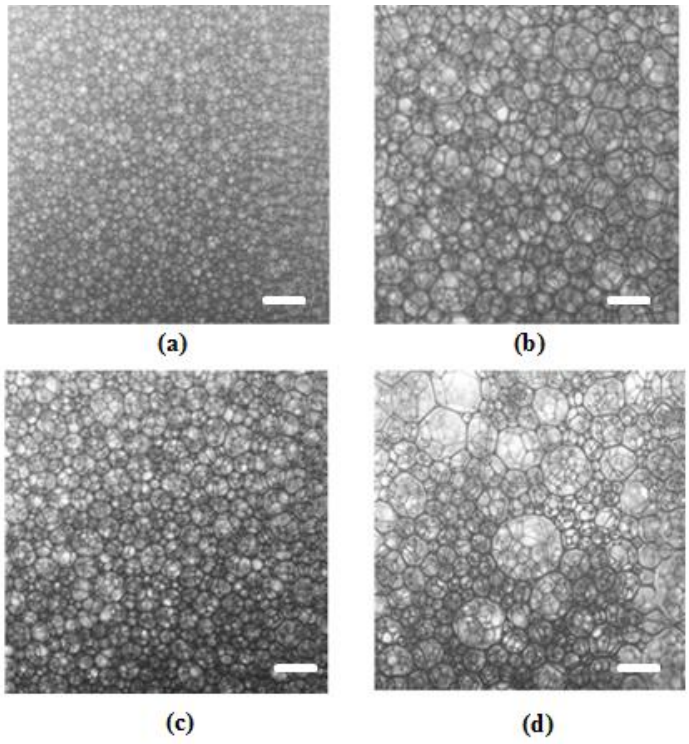

Fig. 8 Microscopic images of AOS and SDS bulk foam (Conc. 0.5 wt %, 298K)

(Scale bar = 200 μm)

Note: a. AOS foam 0s; b. AOS foam 600s; c. SDS foam 0s; d. SDS foam 600s

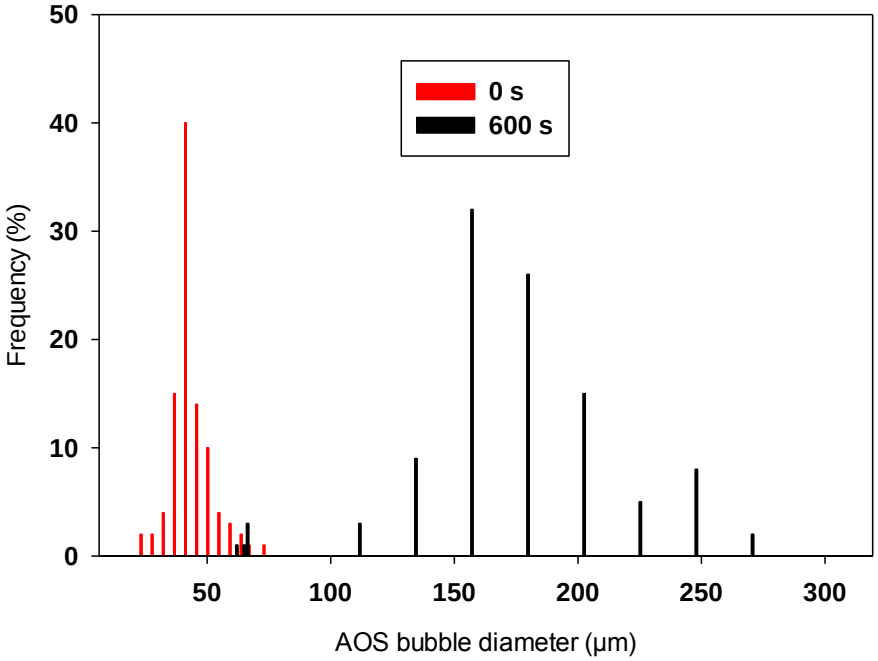

Fig. 9 AOS bulk foam size distribution (Conc. 0.5 wt %, 298K)

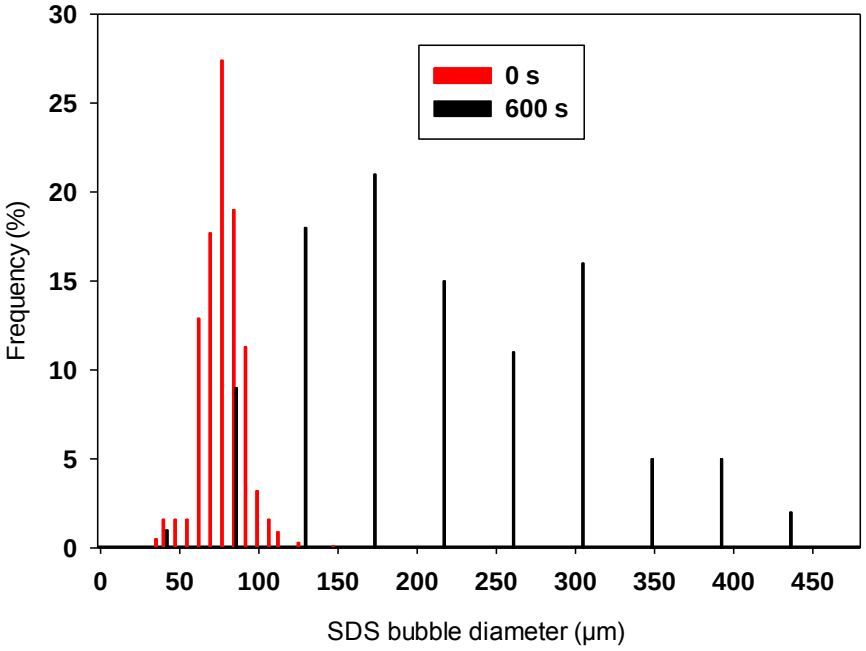

Fig. 10 SDS bulk foam size distribution (Conc. 0.5 wt %, 298K)

3.1.2 Selection of the polymer. Despite its superior foaming ability, AOS alone was not able to secure the foam stability which was critical for practical foam flooding. Therefore, polymer was applied to assist in the improvement of stability. HPAM, the widely used thickener, and AVS, a novel amphiphilic ter-polymer with surface activity, were selected to investigate the influence of polymer type and concentration on foam behavior. The results are presented in Fig. 11-12. Clearly, both foamability and foam stability were closely related to the polymer concentration if the same polymer was added. In general, foamability dropped with an increase in the polymer concentration. Due to the high bulk solution viscosity, AOS molecules would encounter considerable resistance when migrated from bulk solution to the gas/liquid interface, which could detrimentally affect the foaming ability. However, AVS displayed surface activity to some extent just like that of ordinary surfactants, which can be validated by the surface tension measurement in Fig. 13 This resulted in the foamability loss of AOS/AVS foaming solution being less noticeable than that of AOS/HPAM foaming solution due to the introduction of surface active groups which were favorable to the generation of foam. It was also found that the AOS/AVS solution exhibited greater stability compared to the AOS/HPAM solution under the same polymer concentration. This was primarily attributed to the viscosity differences between AVS and HPAM which is illustrated in Fig. 14. Accordingly, AOS/AVS solution was more viscous and had more capacity to reduce the chance of lamella in the foaming system collapsing and decaying, and thus better foam stability could be achieved. For the purpose of balancing foamability and stability, 0.15 wt. % AVS was determined as the most suitable for use in the foaming formulation.

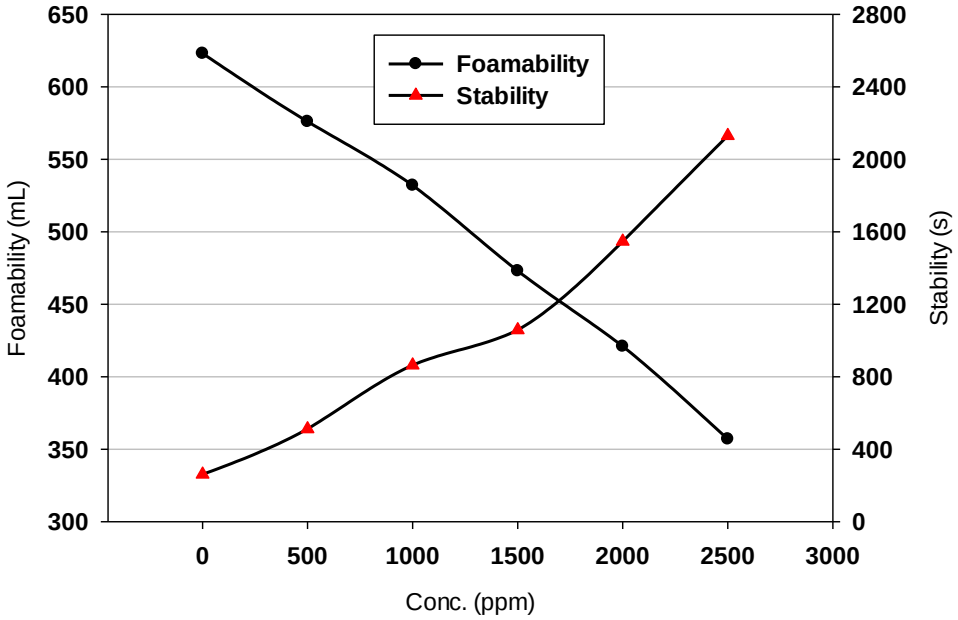

Fig. 11 The dependence of foamability and foam stability on HPAM concentration

(AOS 0.5 wt.%)

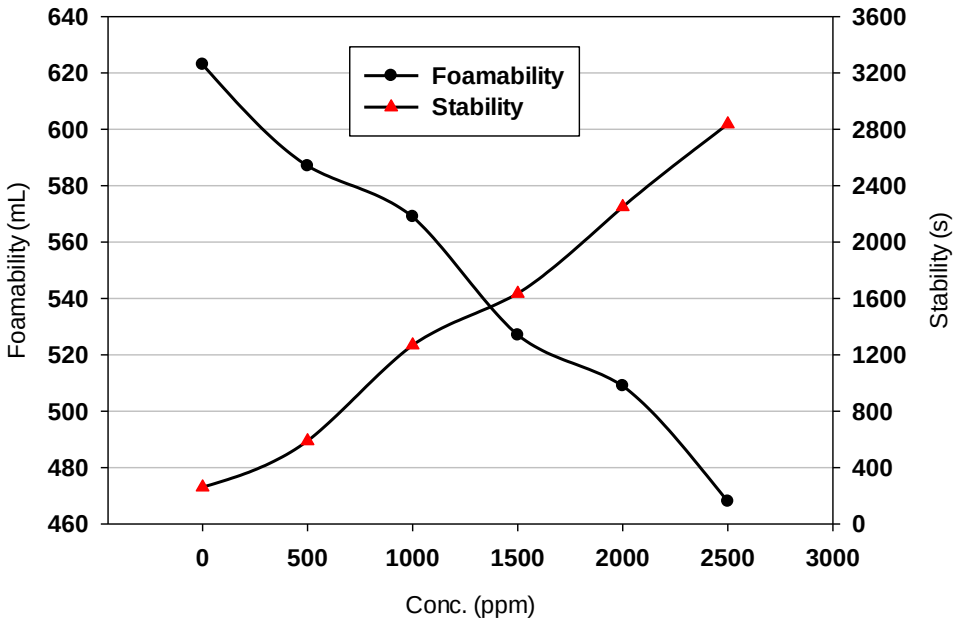

Fig. 12 The dependence of foamability and foam stability on AVS concentration

(AOS 0.5 wt.%)

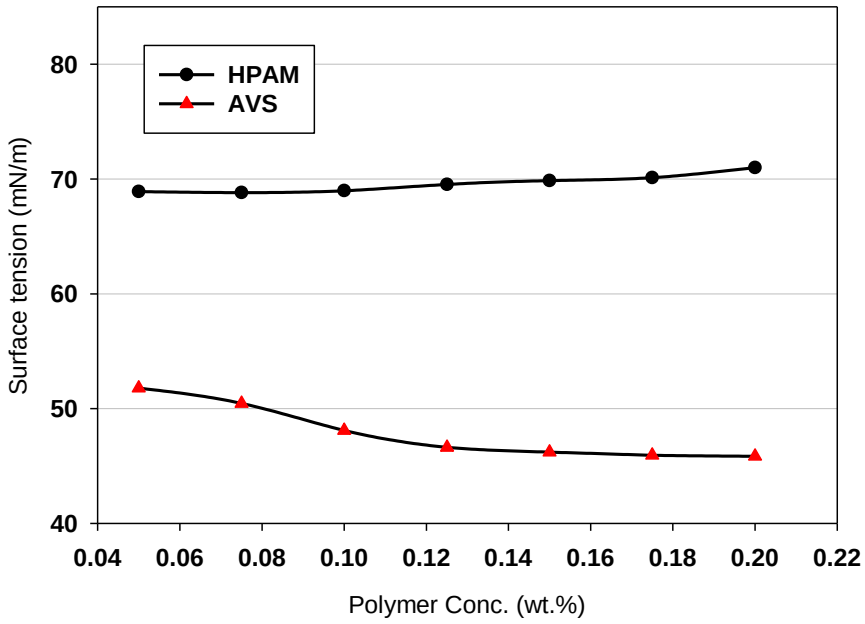

Fig. 13 The effect of polymer concentration on surface tension (293K)

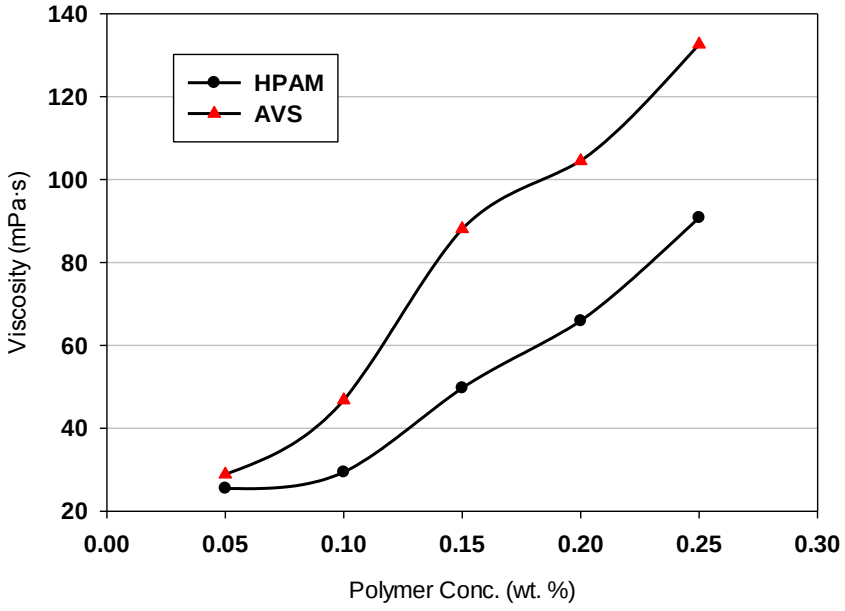

Fig. 14 The effect of polymer concentration on solution viscosity (323K)

3.1.3 Selection of the additive. As mentioned in the early section/earlier, the addition of polymer to the foaming system significantly facilitated the enhancement of the foam stability by improving the bulk solution viscosity and preventing the bubbles from approaching coalescence and breakdown. However, the lamella strength which governed the thinning and rupture of the liquid films separating gas bubbles could not be improved. In this section, the effect of additives called lamella strength booster on the static foam behavior was investigated. Triethanolamine, also known as TEA, which is a viscous compound and another additive N70K-T, a mixture of nonionic surfactant and alcohol were selected as the two alternatives/two options. As shown in Fig. 15, below a concentration of 0.6 wt. %, the lifetime of the foam generated by AOS/AVS/triethanolamine foaming solution increased rapidly as the additive concentration rose until a plateau was reached, while its foaming ability dropped steadily/dropped by the same amount as more boosters were added. Triethanolamine is a compound with strong polarity, and thus it could readily adsorb onto the gas/liquid interface and interact with the existing amphiphilic AVS, which led to the formation of regional micro-network on the liquid membrane, whose rigidity could thereby be enhanced substantially. On the other hand, quantities of AOS molecules were expelled from the interface as a result of the invasion and spatial occupation of the triethanolamine molecules, causing considerable loss of foaming ability; namely, the tremendous boost in foam stability was largely at the cost of its foamability.

The dependence of the foam behavior on another booster N70K-T is illustrated in Fig. 16. Interestingly, a peak appeared on the foamability plot, indicating the optimal foaming performance could be attained under the additive concentration of 0.4 wt. %. As mentioned earlier, N70K-T was a blend of nonionic surfactant and alcohol and both individual substances were added at given concentrations. Sett et al. [23] reported that the foamability of nonionic/anionic surfactant mixture solution could be greater than the foamability of either

of them separately, and they also pointed out that the primary cause of the foamability enhancement might be the higher disjoining pressure which generated thinner but more stable lamella. Thus/Therefore, in this experiment, larger volumes of foam /were created from the mixture solution below an additive concentration of 0.4 wt. %. Still, the foamability declined dramatically beyond the peak and went down to 470 ml. This has arisen from the accumulated alcohol in the solution hampering the association between AOS and nonionic surfactant contained in N70K-T. As for the foam stability, it increased with the N70K-T concentration and was enhanced mainly via two mechanisms: 1) the adsorption of nonionic surfactant molecules onto the gas/liquid interface could rearrange/rearranging/enabling the rearrangement/causing the rearrangement of the ionic distribution on the liquid membrane, which triggered stronger repulsion between bubbles; 2) the interaction between polar alcohol and amphiphilic AVS formed a rigid structure on the liquid membrane. Based on the results obtained above, 0.5 wt. % N70K-T was employed to meet the criteria set for both the foamability and stability. In conclusion, the optimal foaming formulation in this study was determined as 0.5 wt. % AOS + 0.15 wt. % AVS + 0.5 wt. % N70K-T in this research.

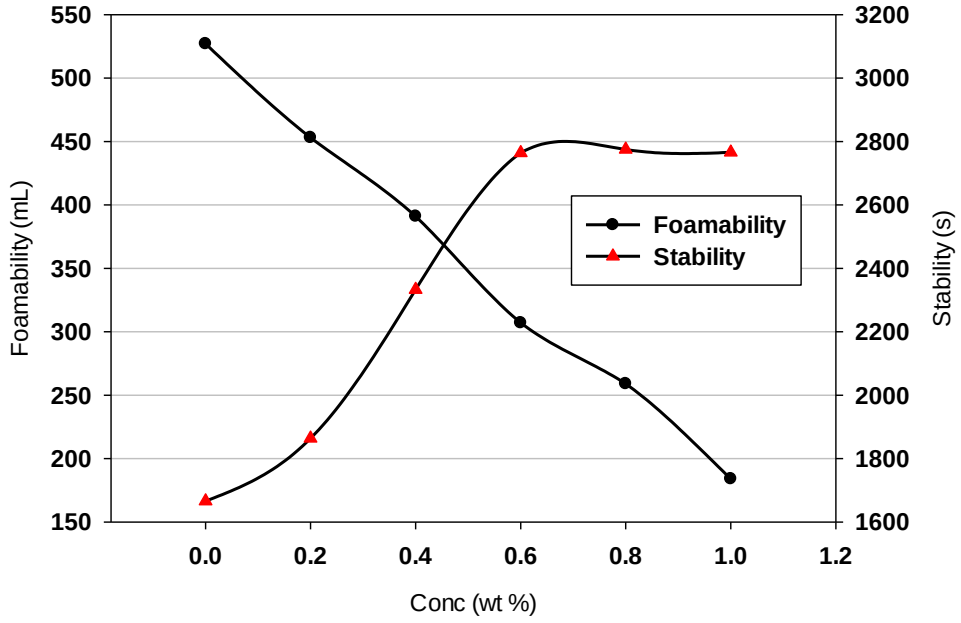

Fig. 15 The dependence of foamability and foam stability on TEA concentration

(AOS 0.5 wt% and AVS 0.15 wt %)

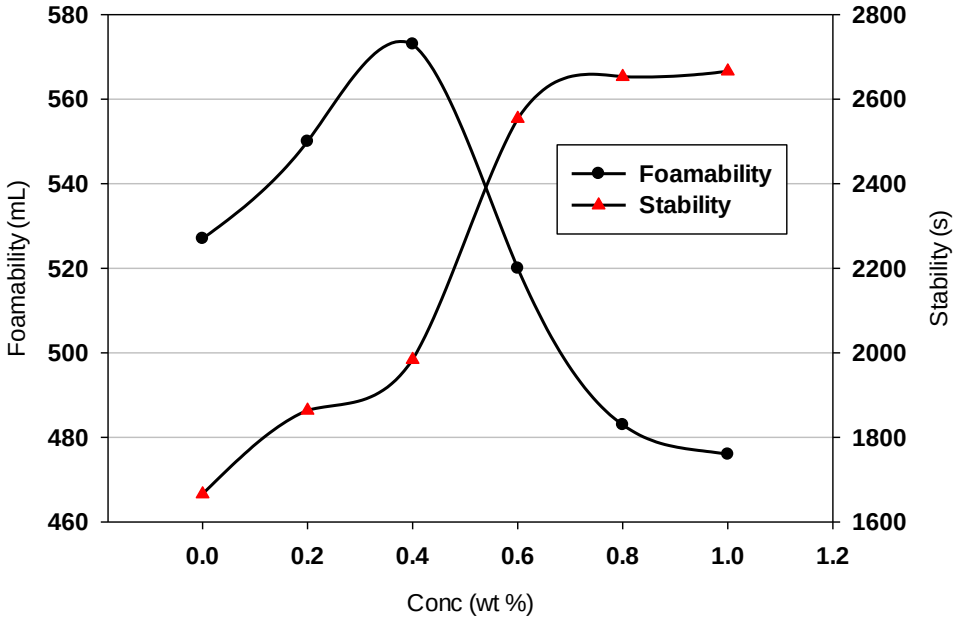

Fig. 16 The dependence of foamability and foam stability on N70K-T concentration

(AOS 0.5 wt. % and AVS 0.15 wt. %)

3.2 Apparent Foam viscosity. In this subsection, apparent foam viscosities were determined in a series of core flooding experiments where a variety of fluid systems (AOS 0.5 wt. %, AOS 0.5 wt. % + HPAM 0.15 wt. %, and AOS 0.5 wt. % + AVS 0.15 wt. % + N70K-T 0.5 wt. %, referred to as formula I, formula II and formula III respectively) and core plugs with different permeability ranges were used. The total superficial velocity (i.e. the sum of liquid flow rate and gas flow rate) was kept constant at 2.0 ml/min, while the foam quality varied from 10% to 95%. The influence of foam quality on the apparent viscosity of foam generated by varying formulations is illustrated in Fig. 17.

Clearly, regardless of the foaming formulation, the maximum apparent foam viscosity always existed under a specific foam quality known as transition foam quality [24] which is indicated by the dash line in all the figures. It seems that the transition foam quality was formula dependent, although the difference between formula II and III was not evident. It was also found that, generally, the apparent viscosity of the foam created by AOS/AVS/N70K-T was the greatest among the three formulations. This could be attributed to its well-balanced foamability and foam stability, which led to the generation of the strongest foam in the experimental conditions. Due to the dramatic loss of (the) foamability or foam stability, the other two formulas exhibited worse thickening performance. Although AOS/HPAM foam was thicker compared to the foam yielded by AOS alone, the difference in viscosity was relatively small. Another intriguing phenomenon was that the apparent viscosity differences among these formulas became less obvious in a low foam quality regime (wet foam) as well as in a high foam quality regime (dry foam), while around the transition foam quality, the viscosity advantage of formula III over the other two was evident.

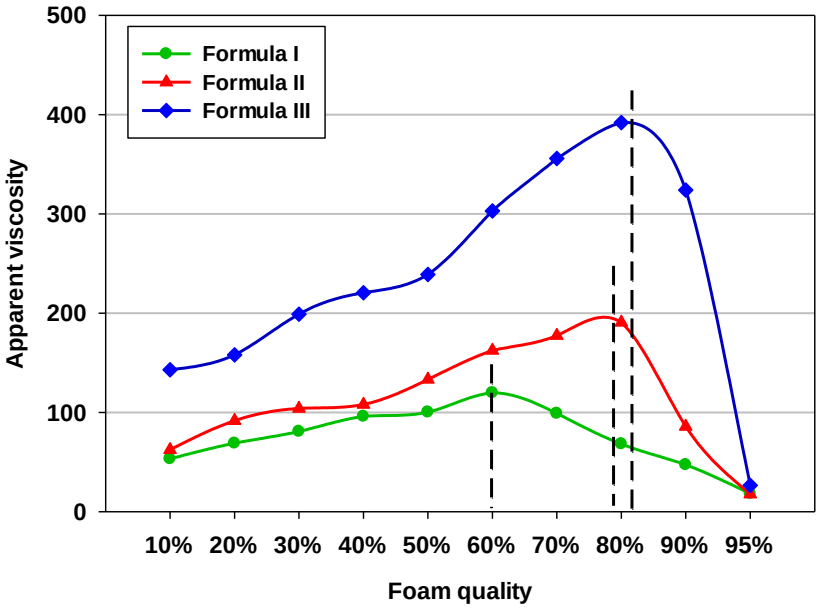

Fig. 17 The influence of the foam quality on the foam apparent viscosity

(323K and 10.3 MPa)

3.3 Resistance factor (RF) and residual resistance factor (RRF) evaluation. As was widely accepted, RF served as a strong indicator of the blockage ability, while RRF suggested the magnitude of relative permeability reduction of the displacing fluid. To evaluate the dependence of RF and RRF on foaming formulation, foam flooding experiments using Formula I, II and III in core plugs with permeability around 450 mD were carried out at 323K and 1500 psi. The results of the experiment are illustrated in Fig. 18.

By comparing the RF and RRF of these foaming formulations, it can be concluded that formula III performed the best in terms of blocking ability as well as changing the relative permeability of the displacing phase. Extraordinary blocking ability led to the improvement of sweep efficiency, and the relative permeability modification promoted the displacement efficiency of the chase brine floods, which could thereby be considered as (the) "extended foam flooding" in terms of its flow behaviour. In other words, the foam generated by foaming formulation III enabled more regions in the core plug to be touched during the displacement of foams and chase brine under the same test conditions compared to the counterpart/alternative formulations I and II.

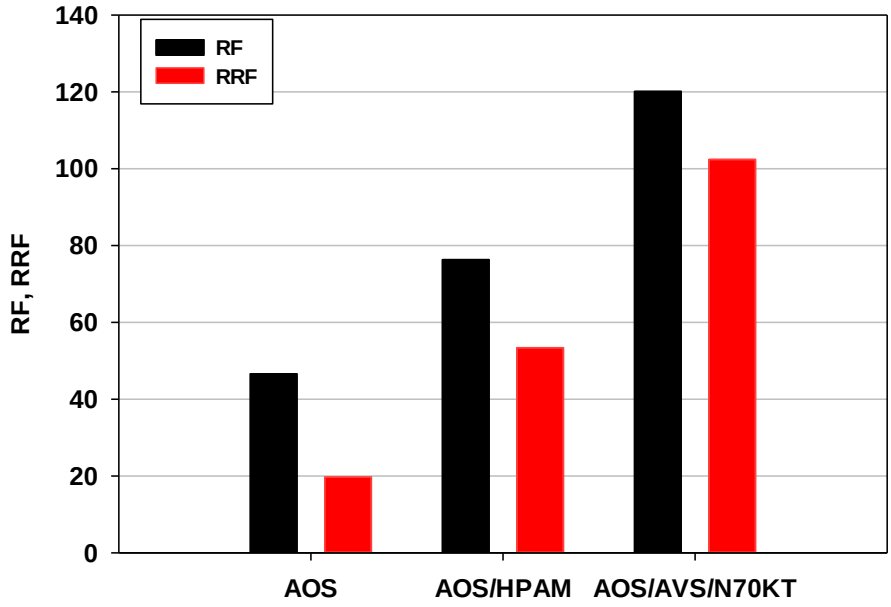

Fig. 18 The RF and RRF of the foaming formulations (323K and 10.3 MPa)

3.4 Accumulative oil recovery. Both the properties of the rock samples and the results of the foam flooding experiments with various formulations are summarized in Table 3. As can be seen, the water floods recovered a comparable amount of the crude oil in each case, but their displacement performances in the water-flooded core plugs were greatly/considerably/quite different: the tertiary oil recovery of formula III was 12.5 % and 6.8% higher than that of formulas I and II respectively, leading to a pronounced difference accumulative oil recovery . As for formula I, its apparent foam viscosity was fairly low due to the unfavourable gas/liquid ratio; furthermore, as stated previously, the foam longevity was detrimentally affected because of the residual oil saturation. Consequently, CO_2 foam induced by AOS alone was not able to improve the oil recovery as significantly as that of the CO_2 foam induced by AOS plus chemicals. In the case of formula II, it recovered more residual oil in the tertiary recovery process than AOS alone due to the presence of the HPAM. However, to some extent, the polymer thermal degradation hindered the positive influence of

the HPAM on CO_2 foams. Therefore, the foams were not as robust as they were supposed to be. Besides, the introduction of the HPAM resulted in a reduced foamability, which also explained its recovery disadvantage. Formula III was endowed with the best displacement performance. The strong degree of synergy between AVS and N70K-T allowed the creation of the extraordinarily reliable lamella and 3D network structure in the solution; therefore, it contributed to the remarkable apparent viscosity and blockage ability. In other words, the sweep efficiency of the displacing phase would be improved substantially as a consequence of the excellent foam flowing performance in the porous media. Further experiments will be performed to investigate the influence of gas/liquid ratio, slug size and foam injection mode on the tertiary recovery of foam flooding in future research.

Table 3 Summary of the oil recovery experiments (323K and 10.3 MPa)

Experiment	#1	#2	#3
Porosity (%)	18.75	17.89	18.63
Brine permeability (mD)	379	369	370
Formula	I	II	III
Gas/liquid ratio	3:1	3:1	3:1
Slug size (PV)	1.0	1.0	1.0
Initial oil saturation (%)	67.0	68.4	68.1
Water floods recovery (%)	33.8	34.6	33.4
Tertiary oil recovery (%)	27.2	32.9	39.7
Overall oil recovery (%)	61.0	67.5	73.1

4. CONCLUSIONS

(1) A number of commercially available surfactants were evaluated in terms of their foamability and foam stability by using the Warring blender method. The nonionic alternatives were unable to produce sufficient amounts of CO_2 foams, although APG foam exhibited the greatest longevity. Anionic foaming agents such as SDS and AOS had similarly

remarkable foaming abilities, but AOS was selected due to its superior foam stability which was validated by the narrow distribution of bubble sizes.

(2) Regardless of the types and concentrations, the addition of polymers and/or lamella booster greatly promoted the foam longevity at the cost of foamability. Both 0.15 wt. % AVS and 0.5 wt. % N70K-T were applied to enhance the foam stability without compromising the foaming ability significantly.

(3) Maximal apparent foam viscosity could be achieved under transition foam quality which seemed to be formulation dependent. The AOS/AVS/N70K-T possessed the highest apparent foam viscosity under the same foam quality among these formulations. However, the viscosity difference became less noticeable in the low and high foam quality areas. It was noted that the apparent viscosity of the foam generated by AOS/AVS/N70K-T was the greatest among the three formulations. This could be attributed to its well-balanced foamability and foam stability and it led to the generation of the strongest foam in experimental conditions.

(4) AOS/AVS/N70K-T foam had extraordinary blocking and relative permeability modification ability, which could be validated by its encouraging RF and RRF.

(5) After water flooding, CO_2 foam enhanced by AVS/N70K-T yielded the most residual oil among the three cases. Its superior displacing performance is believed to be associated with the unique 3D structure that gave rise to the flow resistance when the displacing phase advanced through the porous medium.

ACKNOWLEDGEMENTS

The authors gratefully acknowledge the financial support received from Department of Petroleum Engineering at Curtin University. We also wish to thank the Research Institute of

Petroleum Exploration & Development (Beijing) for providing polymer samples. We should equally express our gratitude to Chao Wang for the help provided in conducting the surface tension measurement and the assistance given by Sarmad Foad Jaber Al-Anssari in the image processing.

REFERENCE

[1] Todd Hoffman, B. and Shoaib, S., 2013, "CO_2 Flooding to Increase Recovery for Unconventional Liquids-Rich Reservoirs," ASME J. Energy Resour. Technol., 136(2), p. 022801.

[2] Wood, D. J., Lake L. W., Johns, R. T. and Nunez, V., 2008, "A Screening Model for CO_2 Flooding and Storage in Gulf Coast Reservoirs Based on Dimensionless Groups," SPE Reserv. Eval. Eng., 11 (03), pp. 513-520.

[3] Martin. D. F., and Taber, J. J., 1992, "Carbon Dioxide Flooding," J. Pet. Technol., 44 (04), pp. 396-400.

[4] Carpenter, C., 2014, "Development of Small-Molecule CO_2 Thickeners," J. Pet. Technol., 66 (07), pp. 145-147.

[5] Guo, X., Du, Z., and Sun, L., 2006, "Optimization of Tertiary Water-Alternate-CO_2 Flood in Jilin Oil Field of China: Laboratory and Simulation Studies," SPE/DOE Symposium on Improved Oil Recovery, Tulsa, Oklahoma, USA, April 22-26, SPE Paper No. 99616-MS.

[6] Holm, L. W., 1982, "CO_2 Flooding: Its Time Has Come," J. Pet. Technol., 34 (12), pp. 2739-2745.

[7] Hild, G.P., and Wackowski, R.K., 1999, "Reservoir polymer gel treatments to improve miscible CO_2 flood." SPE Reservoir Eval. Eng. 2 (02), pp. 196-204.

[8] Akinnikawe, O., Chaudhary, A., Vasquez, O., Enih, C., and Ehlig- Economides, C. A., 2013, "Increasing CO_2-Storage Efficiency Through a CO_2/Brine-Displacement Approach," SPE J., 18 (04), pp. 743-751.

[9] Olabode, A., and Radonjic, M., 2014, "Shale Caprock/Acidic Brine Interaction in Underground CO_2 Storage," ASME J. Energy Resour. Technol., 136(4), p. 042901.

[10] Daneshfar, J., Hughes, R. H., and Civan, F., 2009, "Feasibility Investigation and Modeling Analysis of CO_2 Sequestration in Arbuckle Formation Utilizing Salt Water Disposal Wells," ASME J. Energy Resour. Technol., 131(2), p. 023301.

[11] Heller, J. P., Dandge, D. K., Card, R. J., and Donaruma L.G., 1985, "Direct Thickeners for Mobility Control of CO_2 Floods," Soc. Petrol. Eng. J., 25 (05), pp. 679-686.

[12] Rogers, J.D., and Grigg, R.B., 2001, "A literature analysis of the WAG injectivity abnormalities in the CO_2 process." SPE Reservoir Eval. Eng. 4(05), pp. 375-386

[13] Birarda, G.S., Dilger, C.W., and McIntosh, I., 1990, "Re-evaluation of the miscible WAG flood in the Caroline Field, Alberta." SPE Reser. Eng. 5(04), pp. 453-8

[14] Ren G., Zhang, H., Nguyen, Q., 2013, "Effect of Surfactant Partitioning on Mobility Control During Carbon-Dioxide Flooding," SPE J., 18 (04), pp. 752-765.

[15] Eastoe, J., Paul, A., Nave, S., Steytler, D.C., Robinson, B.H., Rumsey, E., Thorpe, M., Heenan, R.K., 2001, "Micellization of hydrocarbon surfactants in supercritical carbon dioxide." J. Am. Chem. Soc. 123 (05), pp. 988–989

[16] Zanganeh, M.N., 2011, "Simulation and Optimization of Foam EOR Processes," Ph. D. dissertation, Delft University of Technology, Delft, South Holland, Netherlands.

[17] Kutay, S. M., and Schramm, L. L., 2004, "Structure/performance Relationships for Surfactant and Polymer Stabilized Foams in Porous Media," J. Can. Pet. Technol., 43, pp. 19-28.

[18] Khatib, Z. I., and Hirasaki, G. J., and Falls, A. H., 1988, "Effects of Capillary Pressure on Coalescence and Phase Mobility in Foams Flowing through Porous Medium," SPE Reserv. Eng., 3, pp. 919-926.

[19] Worthen, A, Bryant, S., Huh, C., and Johnston, K. P., 2013 "Carbon Dioxide-in- Water Foams Stabilized with Nanoparticles and Surfactant Acting in Synergy," AIChE J. 59 (9), pp. 3490-3501.

[20] Adkins, S. S., Gohil, D., Dickson, J. L., Webber, S. E., and Johnston, K. P., 2007, "Water-in-Carbon Dioxide Emulsions Stabilized with Hydrophobic Silica Particles," R. Soc. Chem., 9 (48), pp. 6333-6343.

[21] Duan, M., Hu, X., Ren, D., and Guo, H., 2004, "Studies on Foam Stability by the Actions of Hydrophobically Modified Polyacrylamides," Colloid Polym. Sci., 282, pp.1292-1296.

[22] Monsalve, A., and Schechter, R. S., 1984, "The stability of foams: The Stability of Foams: Dependence of Observation on the Bubble Size Distribution," J. Colloid Interface Sci., 97(2), pp. 327-335.

[23] Sett, S., Sahu, R. P., Pelot, D. D., and Yarin, A. L., 2014, "Enhanced Foamability of Sodium Dodecyl Sulfate Surfactant Mixed with Superspreader Trisiloxane-(poly) ethoxylate," Langmuir, 30 (49), pp. 14765–14775.

[24] Ma, K., Lopez-salinas, J.L., Puerto, M.C., Miller, C.A., Biswal, S. L., and Hirasaki, G.J., 2013, "Estimation of Parameters for the Simulation of Foam Flow through Porous Media. Part 1: The Dry-Out Effect," Energy Fuels, 27, pp. 2363−2375